

Velocity Spectrum of Protons and Tritons from the d - d Reaction in Scylla*

D. E. NAGLE, W. E. QUINN, F. L. RIBE, AND W. B. RIESENFELD
Los Alamos Scientific Laboratory, University of California, Los Alamos, New Mexico

(Received March 28, 1960)

A diagnostic experiment has been carried out on the d - d reactions produced by fast magnetic compression of a deuterium plasma. A determination of the velocity spectra of protons and of tritons from the d - d reaction was made by magnetic analysis and nuclear plate detection of the particles. The observed distributions are Gaussian, with widths which correspond to a deuteron temperature of 1.3 kev. Comparison of the mean proton and triton momenta indicates that no plasma drift in the (axial) direction of observation is present, nor any potential difference between the source plasma and detector greater than a few volts. These results, coupled with previous ones on the neutron yield, duration, source extent, and lack of circumferential drift argue against any of the simple, physically plausible non-Maxwellian acceleration mechanisms for the d - d reactions so far proposed.

INTRODUCTION

SCYLLA, the Los Alamos experiment on fast magnetic compression of a plasma, has been shown to produce about 10^7 neutrons per pulse from the reaction $D(d,n)He^{3,1,2}$. An equivalent ion temperature of about 1.5 kev corresponding to this yield can be computed, using our measured values of the ion density, volume of the emitting region, and mean duration of the neutron pulse, as well as the previously measured values of the d - d cross section. As has often been remarked, however, temperatures based on the reaction rate alone deserve little credence until the rate is so high as to be inexplicable on any other assumption than the thermal one.

The other branch of the reaction, namely $D(d,p)T$, produces 3-Mev protons and 1-Mev tritons, particles which are conveniently detected with nuclear emulsions.³ Problems of the origin of these d - d reactions, whether thermonuclear or from acceleration by electric fields, have been studied using these reaction products, both charged and neutral. Cranberg and Boyer have emphasized the improved resolution possible by using magnetic analysis of the charged products.⁴

If we have a thermal plasma at a temperature T , the velocity distribution of the d - d reaction products is nearly gaussian if kT is small compared to the reaction Q value, and the width of the gaussian is proportional to the square root of T . It is a good approximation to say that the width is the rms velocity of the center of mass of the d - d system. For temperatures high enough to give appreciable reaction yields, the width is easily measurable, the precision depending on statistics rather than on the resolving power of our experimental arrangement.

Comparison of the spectra of the protons and the tritons affords a test for consistency of the thermal hypothesis. In addition if there are mass motions of the plasma, they can be determined from the difference of the mean values of the two momentum distributions.

We find for the first model of Scylla an ion temperature of 1.3 ± 0.2 kev.⁵ No mass motions in the axial direction are observed. The velocity spectra obtained, coupled with the lack of observable mass motion in either the radial² or axial direction, argue against many of the mechanisms for spurious, nonthermal, d - d reactions.⁶

THE VELOCITY SPECTRUM

We consider a hot homogeneous plasma for which the velocity distribution function is $f(\mathbf{v})$. The probability that a pair of ions have a relative velocity \mathbf{v}_r and a center-of-mass velocity \mathbf{v}_c is $f(\mathbf{v}_c + \frac{1}{2}\mathbf{v}_r)f(\mathbf{v}_c - \frac{1}{2}\mathbf{v}_r)$, and the inelastic collision rate per unit volume for ion density n_d is

$$d^6N = \frac{1}{2}n_d^2 v_r \sigma(v_r) f(\mathbf{v}_c + \frac{1}{2}\mathbf{v}_r) f(\mathbf{v}_c - \frac{1}{2}\mathbf{v}_r) d^3\mathbf{v}_r d^3\mathbf{v}_c. \quad (1)$$

The product of the normalizable f factors above separates into a product of functions involving only \mathbf{v}_c and \mathbf{v}_r if and only if $\ln f(\mathbf{v})$ is a quadratic form in the components of \mathbf{v} ; normalizability requires that this form be negative definite. If f is gaussian in the components of \mathbf{v} , the product becomes a product of Maxwellian distributions in \mathbf{v}_c and \mathbf{v}_r . The average of σv_r is gotten by integrating this expression over all velocity space. The experimental cross sections for the $D(d,p)T$ and $D(d,n)He^3$ reactions are given by Arnold et al.⁷ Their results for the cross section for both these reactions

* Work performed under the auspices of the U. S. Atomic Energy Commission.

¹ W. C. Elmore, E. M. Little, and W. E. Quinn, Phys. Rev. Letters **1**, 32 (1958).

² K. Boyer, W. C. Elmore, E. M. Little, W. E. Quinn, and J. L. Tuck, this issue [Phys. Rev. **119**, 831 (1960)].

³ T. E. Allibone, D. R. Chick, G. P. Thomson, and A. A. Ware, *Proceedings of the Second United Nations International Conference on the Peaceful Uses of Atomic Energy, Geneva, 1958* (United Nations, Geneva, 1958), Vol. 32, p. 169.

⁴ L. Cranberg (private communication).

⁵ For preliminary accounts of the present experiments see D. E. Nagle, W. E. Quinn, W. B. Riesenfeld, and W. Leland, Phys. Rev. Letters, **3**, 318 (1959); See also articles by F. L. Ribe and J. L. Tuck, in *4th International Conference on Ionization Phenomena in Gases, Uppsala, Sweden* (North Holland Publishing Company, Amsterdam, 1960).

⁶ O. A. Anderson, W. R. Baker, S. A. Colgate, J. Ise, and R. V. Pyle, Phys. Rev. **110**, 1375 (1958).

⁷ W. R. Arnold, J. A. Phillips, G. A. Sawyer, E. J. Stovall, and J. L. Tuck, Phys. Rev. **93**, 483 (1954).

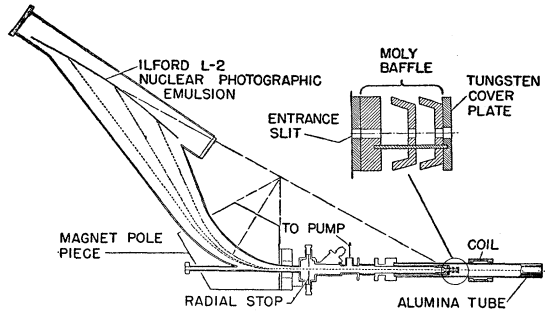


FIG. 1. Experimental arrangement for measuring the spectra of protons and of tritons from the d - d reaction in Scylla. The reactions have been shown to occur in a region of volume 3 cm^3 near the center of symmetry for the coil. The charged tritons and protons enter the spectrometer through a slit and follow the trajectories shown as dotted lines.

may be summarized as follows:

$$\sigma_{dd} = (A/E) \exp(-BE^{-1/2}), \quad (2)$$

where for energies less than 10 keV A has the value $187 \times 10^{-24} \text{ cm}^2 \text{ keV}$ and B the value $44.2 (\text{keV})^{1/2}$; for energies greater than 10 keV A equals $288 \times 10^{-24} \text{ cm}^2 \text{ keV}$ and B equals $45.8 (\text{keV})^{1/2}$.⁸ The average of $\sigma_{dd}v$ over a Maxwell distribution we denote by $\langle \sigma v \rangle_{av}$. One finds approximately

$$\langle \sigma v \rangle_{av} = CT^{-3/2} \exp(-DT^{-1/2}), \quad (3)$$

where the corresponding values of C and D are, respectively, $240 \times 10^{-16} \text{ cm}^3/\text{sec}$ and 18.6 at low energies and at high energies $370 \times 10^{-16} \text{ cm}^3/\text{sec}$ and 19.2 . The observed velocity spectrum of protons in the laboratory system is obtained by integrating d^6N with the constraint $\mathbf{v}_p = \mathbf{v}_1 + \mathbf{v}_c$ where v_1 is the proton speed in the center-of-mass system. The reaction products are assumed to be distributed isotropically in the center-of-mass system. The result for a plasma with ion temperature T is

$$\frac{dN}{dE} = \frac{n_d^2 \langle \sigma v \rangle_{av}}{m_p v_0} \left(\frac{m_d}{4\pi kT} \right)^{3/2} \exp \left[-\frac{m_d}{kT} (v - \bar{v})^2 \right], \quad (4)$$

where for the protons,

$$\frac{m_p v_0^2}{2} = \frac{m_t}{m_p + m_t} Q, \quad (5)$$

and

$$\bar{v} = v_0 \left[1 + \frac{kT}{2Q} \left(\frac{d \ln \langle \sigma v \rangle_{av}}{d \ln kT} + \frac{3}{2} \right) \right]. \quad (6)$$

The triton velocity spectrum is obtained from the above expressions by interchanging the subscripts p and t . The logarithmic derivative is about 4.5 at $kT = 1 \text{ keV}$, so that \bar{v} is about 0.1% larger than v_0 . Terms quadratic in this deviation have been omitted in the above expressions.

⁸ E. J. Stovall, Jr. (private communication).

According to expression (4) the shape of the distribution is gaussian, with a width depending on T and m_d only. The effect of dependence of the cross section on energy, in the present approximation, is merely to shift slightly the center of the distribution. The Q value of the reaction is $4.022 \pm 0.016 \text{ MeV}$, corresponding to $v_{op} = 2.4078 \times 10^9 \text{ cm/sec}$ (1 ± 0.002) and $v_{ot} = 8.0429 \times 10^8 \text{ cm/sec}$ (1 ± 0.002).

EXPERIMENTAL ARRANGEMENT FOR MEASURING THE SPECTRUM

The axial direction was chosen for a first experiment because no window in the side of the discharge tube is required, and because the interpretation of the data is somewhat simpler. The rest of the geometry was fixed by the parameters of a magnetic spectrograph which was available. The Scylla discharge takes place inside the alumina tube at the center of the coil. The region from which the neutron, proton, and x-ray emission appears to come is roughly spheroidal of diameter 15 mm and length 21 mm.^{2,9} The entrance slit is placed as close as possible to the discharge, the practical limitation being that the slit, if too near the discharge is damaged by heat and wall material which strike it during late stages of the discharge. Several trials resulted in the design of the protective baffle shown in Fig. 1 with

TABLE I. Spectrograph exposures.

A. Scylla G operation	First	Second
Tube	Alumina	Alumina
Pressure	90 μ	90 μ
Bank voltage	85 kv	85 kv
No. of discharges	1617	1888
Total neutrons (measured by silver counter)	$(0.992 \pm 0.06) \times 10^{10}$	$(1.13 \pm 0.07) \times 10^{10}$
B. Spectrograph operation		
Magnetic field intensity	$6.762 \times 10^3 \text{ gauss}$	$6.762 \times 10^3 \text{ gauss}$
f_{res}	$28.00 \times 10^6 \text{ cps}$	$28.00 \times 10^6 \text{ cps}$
Standard radius of curvature	40.0 cm	40.0 cm
Deflection (standard)	60°	60°
Energy of proton of standard radius	3.20 Mev	3.20 Mev
Entrance aperture	5 mm diam circle located 2 in. from edge of coil, on the axis	Rectangle 2.5 mm \times 6 mm
Line of sight	Centered on coil center	1.2 mm toward feed point of coil
C. Type of plate		
Ilford L -2	100 μ thick, 3.92 g/cm ² with extra plasticizer	100 μ thick, 3.92 g/cm ² with extra plasticizer
Protective foil	1 mg/cm ² polyester double aluminized	0.55 1mg/cm ² grade A nickel

⁹ F. C. Jahoda, E. M. Little, W. E. Quinn, G. A. Sawyer, and T. F. Stratton, preceding paper [Phys. Rev. 119, 843 (1960)].

TABLE II. Range identification of tracks, Plate S-4.

H Horizontal position on plate (mm)	E Energy from calibration (Mev)	N No. of tracks	L_{av} Projected range (μ)	SL Rms deviation (μ)	ϕ Dip angle (calculated)	L^* True range (μ)	R From range energy relation (μ)
33.9 to 38.7 Av=36.3	2.909	72	57.31	3.19	25°30'	70.42	71.5
88.1 to 88.7 Av=88.4	3.082	58	63.95	2.93	25°3'	77.7	78.4

which the erosion of the slit is negligible. The slit was 10 cm from the center of the discharge.

The entrance slit forms the object for the ion optical system shown in Fig. 1, and the image is formed at the nuclear plate. A "radial" stop near the entrance to the magnet limits the angle in the plane of figure to 0.01 radian, and in the plane normal to the plane of the figure the angle is limited to 0.01 radian by the vacuum chamber walls.

Table I gives some characteristics of the mass spectrograph. Details of its design, which was done by Leland, will be published elsewhere. The magnetic field of the spectrograph is held constant by controlling the current in the magnet windings from a servo amplifier operating on the proton resonance frequency. An independent proton resonance unit was used to monitor the field visually. The observed magnetic field fluctuation during a data run was less than one part in 10^5 .

SPECTROGRAPH PLATE EXPOSURES AND SCANNING

In the initial phases of the experiment we searched for the emergent protons using instead of the spectrograph a simple pinhole camera. A pinhole 2.5 mm in diameter was located at 12.5 cm from the center of the discharge. At 7.7 cm on the opposite side of the pinhole a nuclear emulsion was located inclined at 40° to the axis of the discharge tube. The plate was exposed for 180 discharges. Upon development and scanning, the 3-Mev proton tracks were easily identified in the manner discussed below. By plotting the tracks per unit area found on the plate we obtain an image of the emitting source. The diameter is approximately 15 mm which is in good agreement with the neutron collimation experiment,² and soft x-ray pinhole photographs.⁹ The density is roughly uniform throughout the image, falling off monotonically from the center. A computer study of the trajectories to be expected showed that the magnetic field reduces the image size by a few percent, and this correction has been applied above. The density of tracks indicated that the yield was lower by approximately a factor of 3 than that determined by the neutron silver-counter detector. This discrepancy is not understood.

Two runs were made with the spectrograph and charged particles from Scylla. The second differed from the first mainly in the use of a narrower entrance slit

and a thinner protective metal foil covering the emulsion. The essential data are given in Table I. The discharge tube pressure was 90 μ of D_2 gas, and the voltage on the condenser bank 85 kv. The resonance frequency f_{res} was that of the proton magnetic moment.

The neutron yield as measured by the silver counter was recorded for every discharge. The total number of neutrons during the exposure of each plate is listed in the fifth row of Table I with its standard deviation.

The first plate after development showed a large number of tracks having the following properties: (a) Their projected range was between 55 and 75 microns. (b) They entered the emulsion at about 24° to the emulsion. (c) On entering they were parallel to the long axis of the plate. (d) The grain density of the track was roughly consistent with 3-Mev protons. The tracks all came in the region of the plate where 3.0 ± 0.2 Mev protons should appear. Accordingly they are identified with the protons from the $d-d$ reaction (energy 3.022 Mev).

Further details of the identification of two selected groups of tracks according to range are shown in Table II. One group of tracks was chosen to lie between 88.1 and 88.8 mm on the plate, with an average position 88.4 mm. This position, according to an energy vs position calibration previously done with a beam from an electrostatic generator, corresponds to 3.082-Mev energy for protons. The projected range was $63.95 \pm 2.93 \mu$, the rms deviation being partly due to errors in measurement of projected range and partly due to straggling. It will be demonstrated that the spectrograph itself contributes negligible spread. This range is divided by the cosine of 25.3°, the angle of dip, to get the true range in the emulsion. To this must be added 7 μ , the path length equivalent of the protective foil covering the emulsion to get the total observed range of 77.7 μ . This agrees with the value 78.4 μ expected from the range energy relation for 3.08-Mev protons in Ilford L-2 emulsion. A similar situation is shown in Table II for a second position on the plate, where the agreement is again good. One can already see from Table II that the spread of the track distribution genuinely indicates an energy spread in the beam. We concluded that these indeed are the protons from the $d-d$ reaction, and we adopted the following criteria for scanning: (a) The range is between 55 and 80 microns. (b) Their dip is roughly consistent

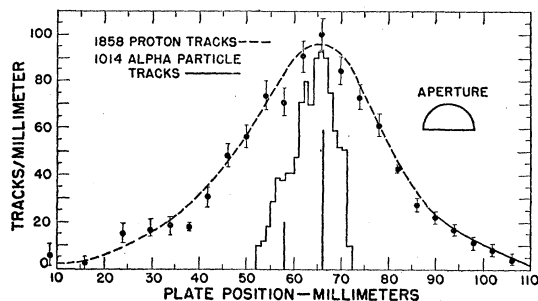


FIG. 2. The experimental track distribution from Scylla is shown in the dashed curve. The solid histogram is the result of a calibration with Pu^{240} alpha particles, performed to check the energy calibration and the resolution of the instrument. The resolving power is determined by the finite width of the entrance slit.

with 25° entry. (c) They enter the emulsion going from left to right and parallel to the long axis of the plate within $\pm 10^\circ$. (d) The grain density is about right.

With these criteria the plate (2 in. \times 10 in.) was scanned from one end to the other. Figure 2 shows the observed distribution, based on 1858 tracks. About 40 tracks were rejected. Most of these came from cosmic-ray stars in the emulsion, or else went clear through the emulsion. The number of tracks found per unit area at a given location along the plate is plotted as a function of the location along the plate. (It happens that the energy of the particle at this position is very nearly a linear function of distance along the plate to the track, the rate of change having approximately the value 3 kev/mm).

From analytical geometry considerations, one computes that the effective resolution of the spectrograph is set essentially by the width of the entrance slit suitably projected on the image plane. This is shown as the semicircle in Fig. 2. One sees that the proton distribution is much wider than the resolution width.

As a further experimental check *in situ*, plates were exposed using the alpha particles from separated Pu^{240} isotope. There are two main alpha lines for this isotope, of energies 5.118 Mev and 5.162 Mev and of relative intensities 1 and 3.1, respectively. Their computed separation is shown in Fig. 2 by means of the vertical bars, and the histogram shows the observed alpha particle distribution. Although the lines are not resolved, the observed distribution is consistent with the quoted resolution. One concludes therefore that the observed width of the proton distribution is not instrumental in origin.

The second plate (Fig. 3) shows the same distribution, but with the improved resolution the results are more dramatic. Again an alpha particle exposure was made; this time the alpha lines are clearly resolved. The energy separation of the alpha lines, 44 kev, corresponds to 28 kev on the proton energy scale. The predicted resolution is 9 kev. The protective nickel foil (0.55 mg/cm²) was thin enough to allow the tritons to register on the plate with a residual range of 5 microns. A total of

2569 protons and 2138 tritons were found. Figure 3 shows the track distributions of protons, alphas, and tritons. The smaller number of tritons may reflect some scanning loss for these particles. The triton curve is seen to be about three times wider than the proton curve, a consequence of the triton to proton mass ratio.

The reduction of these curves to distributions in velocity, and their comparison with the expression (1) is given in the following section.

REDUCTION OF THE DATA TO VELOCITY DISTRIBUTION

Figures 2 and 3 have as ordinate the number of tracks found by the scanners, and as abscissa location of the track, measured in mm along the plate. We transform the ordinate into number of particles per unit of energy and the abscissa into particle velocity. This transformation is done analytically, starting with the spectrograph parameters. The transformation of the ordinate involves computing the variation along the plate of lateral magnification, length of the trajectory, and angle of incidence of the tracks. In the interval between the half-value points of the proton distribution, the order of magnitude of these corrections is as follows: The energy calibration is linear to one half percent, and the track density function is changed by five percent.

An experimental check of this computation was made using the Pu^{240} alpha source and several magnetic field settings. In this way we found that the energy scale was shifted by 12 kev for protons. This we attribute to imperfect alignment of the axis of Scylla with the spectrograph axis. The alpha calibration was adopted as standard. The density function was measured by making time exposures with alpha particles for two different magnetic field values. We found that the density function measured in this way differed from the prediction by an amount which would introduce an uncertainty of one half percent in making the above correction. The principal effect of this reduction on our distributions is to

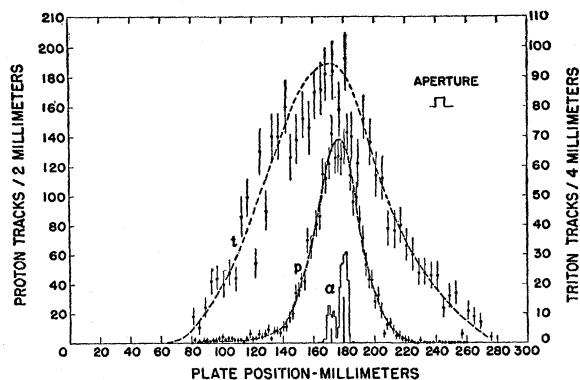


FIG. 3. Track distribution for the second exposure. The thinner protective cover on the emulsion permits the tritons to be detected. The Pu^{240} α particles used for calibration are seen to be well resolved. The triton curve is wider than the proton curve because of the greater mass of the tritons.

shift the mean velocities slightly toward higher energy. The widths of the distributions are little changed.

Figures 4 and 5 give the results for the first and second exposures, respectively. One notices immediately that the widths of the proton and triton distributions are very closely the same. The solid curves are computed from Eq. (4) for the values $T=1$ and 1.5 kev as indicated. The curves do not pass through the 20 anomalously low-energy proton tracks, which may result from scattering off the edge of the slit. In Fig. 4 the value of \bar{v} was chosen to be the computed value of 2.412×10^9 cm/sec for 1 kev, and 2.411 for 1.5 kev. The peak of the observed distribution is about 2.411×10^9 cm/sec. The discrepancy is within the quoted error for the Q value of the reaction. For the second plate, Fig. 5(A), the center of the solid curves was chosen for best fit, namely 2.412×10^9 cm/sec. For the tritons, Fig. 5(B), the predicted \bar{v} is 0.8057×10^9 cm/sec and the observed mean of the distribution is 0.8041×10^9 cm/sec. Inspection of these curves indicates that a temperature of about 1.3 kev gives a good fit to all the data.

The results of the mean velocity determinations may be summarized in the following way: In the absence of any motion of the gas as a whole toward the observer, Eq. (6) predicts $\bar{v}_p/\bar{v}_t = m_t/m_p = 2.994$. Experimentally $\bar{v}_p/\bar{v}_t = 2.999 (1 \pm 0.005)$ where the error quoted is a statistical one. An error in the absolute energy scale does not affect the ratio. The discrepancy in these values would correspond to an energy in the mass motion of only a few electron volts.

DISCUSSION

The most straightforward interpretation of the velocity spectra is that the $d-d$ reactions arise from collisions in a plasma with an ion temperature of 1.3 ± 0.2 kev. An uncertainty in fitting the temperature is introduced by the low-energy tail to the proton distribution. However, this tail involves only about 1.5% of the reactions and might be accounted for by slit effects or by a streaming of a small portion of the plasma away from the direction of observation.

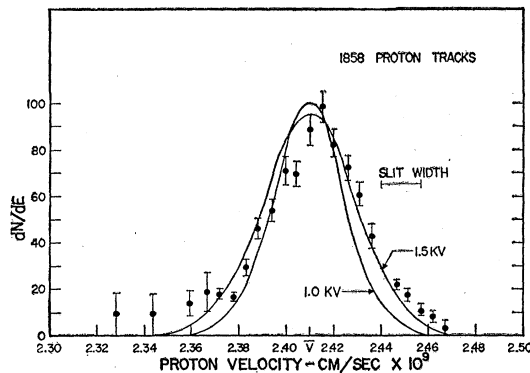


FIG. 4. Velocity spectrum of protons, from the first plate. The solid curves are computed from the expressions given in the text.

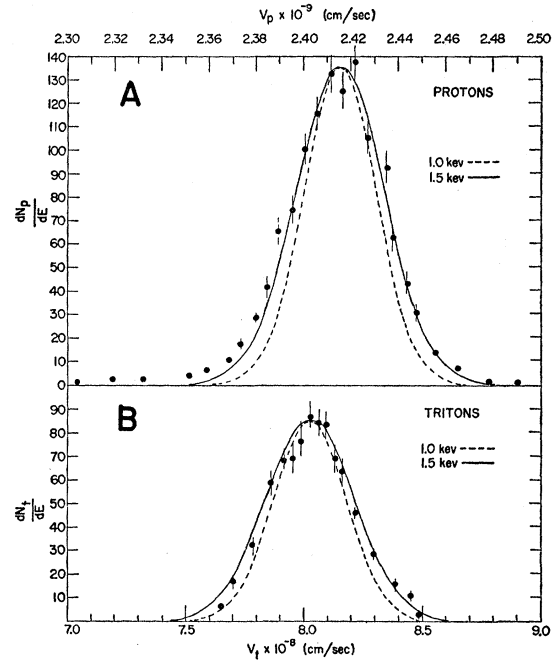


FIG. 5. Velocity spectra of protons and of tritons, from the second plate. The curves are computed from expressions given in the text. A temperature of about 1.3 kev for the deuterium ions is inferred from these data and from the data of Fig. 4.

A streaming in the axial direction of the plasma as a whole would manifest itself as a shift of the mean velocity from the value predicted by Eq. (6) for both protons and tritons, and if such a shift exists it is below the experimental sensitivity of 5 parts in 10^4 . The existence of an electrostatic sheath near the plasma boundary would also generate velocity shifts, and the fact that these would be different for protons and tritons renders them even more amenable to experimental detection. The experimental spectra place an upper limit of a few ev on the magnitude of such sheath-induced energy shifts.

There remains, of course, the question of the uniqueness of our interpretation of the spectra. While a given velocity distribution of the reactant (deuteron) particles leads to a unique product particle (proton and triton) distribution, the converse is not the case. Therefore, the procedure to be followed in analyzing the data consists of making educated guesses about the form of the deuteron distribution and comparing the calculated resultant charged particle distribution with the experimental one. The forms of the assumed deuteron distributions are dictated by possible physical models describing the heating or accelerating mechanisms in Scylla during the first two half-cycles. Most distributions in which an appreciable fraction of the nuclear reaction rate is caused by the relative motion of two deuteron groups with different mean velocities are decisively ruled out by the data. No explicitly calculated model of this type could simultaneously account for the

shape of the reaction product distributions and the yield. More difficult to rule out is a model which would vary the relative velocity vector between the two groups from discharge to discharge, corresponding to a random acceleration mechanism. The center-of-mass velocity vectors of the groups could conceivably be made to vary in such a way that the average over many discharges reproduces the distributions of Figs. 4 and 5. This interpretation, however, seems contrary to other evidence, for example the reproducibility of the neutron yield versus time curve^{1,2} which argues against a mechanism which differs between successive discharges.

At this point, we compute the ion temperature which is necessary to account for the neutron yield as measured in this experiment. The average neutron yield Y was $(6.0 \pm 0.36) \times 10^6$ per discharge. The statistical error quoted above we believe to be small in comparison with the uncertainties in the silver counter calibrations arising from geometry and room scattering, which we estimate to be as large as a factor of 2. The volume V of the emitting region can be determined from the neutron, proton, and x-ray images to be $3.0 \pm 1.5 \text{ cm}^3$.^{2,9} The ion number density n has been determined by studies of the electromagnetic radiation⁹ to be $(4.3 \pm 1.7) \times 10^{16} \text{ cm}^{-3}$. The mean time of neutron emission Δt , $(0.9 \pm 0.2) \times 10^{-6} \text{ sec}$, is based on oscillogram records from a plastic scintillation neutron detector.² The neutron yield is given by

$$Y = \frac{1}{2} n^2 \langle \sigma v \rangle_{av} V \Delta t. \quad (7)$$

Using Eqs. (7) and (3) we find $T = (1.5_{-0.4}^{+0.3}) \text{ kev}$. This is in satisfactory agreement with the spectral temperature value quoted above.

The only models quantitatively consistent with the data seem to be those which produce most of the nuclear yield as a consequence of randomized deuteron motion. This does not necessarily imply that the deuterons are in true thermal equilibrium. For the time scale and densities involved, the ions are certainly not in thermal equilibrium with the electrons, and the time available for ion-ion collisional equilibrium is marginal. But a Maxwellian deuteron distribution with fixed, isotropic temperature is the simplest and mathematically most tractable model to try and leads to results remarkably in accord with the data by fitting only one parameter, the temperature. Additional valuable information would undoubtedly be obtained by examining timeresolved distributions which might display such effects as cooling and relaxation of the ions.

If a distribution could be obtained from a single discharge, as for example by using the larger yield obtainable from the d -T reaction, the possibility of the gaussian distribution having been simulated by the

summation of random events, as discussed above, could be ruled out.

We have seen that the ion temperature determined from the proton and triton spectra is consistent with that deduced from the neutron yield. It remains to determine if the requirement of pressure balance between the plasma particles and the external magnetic field is satisfied. The plasma pressure is given by $\sum n_i k T_i$ where the summation extends over all particle species present at their respective temperatures. The electromagnetic radiation measurements⁹ have shown that at peak magnetic compression: the electron density $n_e = (5 \pm 1) \times 10^{16} \text{ cm}^{-3}$, the electron temperature $T_e = 240 \pm 40 \text{ ev}$, the deuteron density $n_d = (4.3 \pm 1.7) \times 10^{16} \text{ cm}^{-3}$, and the oxygen impurity ion density $n_o = (9 \pm 4) \times 10^{14} \text{ cm}^{-3}$. Taking the deuterons and oxygen ions to have the same temperature $T = (1.3 \pm 0.2) \text{ kev}$, we find the following partial pressures: $p_e = (1.9 \pm 0.6) \text{ joule cm}^{-3}$, $p_d = (8.9 \pm 3.2) \text{ joule cm}^{-3}$, $p_o = (0.2 \pm 0.1) \text{ joule cm}^{-3}$. The total particle pressure is $(11.0 \pm 3.3) \text{ joule cm}^{-3}$.

Vacuum probe measurements² show that the magnetic field at the time of peak compression during the second half-cycle is $(56 \pm 4) \text{ kgauss}$ in the mirrors and $(49 \pm 3) \text{ kgauss}$ at the midplane. In estimating the magnetic pressure $B^2/8\pi$ with plasma present we use the value $(56 \pm 4) \text{ kgauss}$, since the mirror magnetic field is not affected by the plasma, and obtain a magnetic pressure of $(12.5 \pm 1.8) \text{ joule cm}^{-3}$. Comparing with the plasma pressure value of $(11.0 \pm 3.3) \text{ joule cm}^{-3}$, we see that the requirement of pressure balance is satisfied within experimental error. The ratio β of particle to magnetic pressure in a magnetic confinement experiment could *a priori* lie between zero and unity. The above result indicates that in Scylla the particle pressure approaches the maximum that can be attained.

ACKNOWLEDGMENTS

We acknowledge with pleasure the contributions of Louis Rosen's microscopy group, especially those of Mrs. Delia Loewenstein and Mrs. Bertha Longsine. We thank Edward M. Little and Winthrop W. Smith for their assistance in setting up the experiment and in operating Scylla. We are indebted to W. T. Leland for the loan of the spectrograph and his assistance in its application to this experiment. Roy Olsen contributed generously of his time and experience in helping us set up and operate the spectrograph. We thank Lawrence Cranberg for a communication which first aroused our interest in this experiment. The help of many members of the Los Alamos Sherwood Project was freely given and is gratefully acknowledged.